Identification of Dihydropyrazolo[1,5-*a*]pyrazin-4(5*H*)-ones as Cyclic Products of β-Amidomethyl Vinyl Sulfone Alphavirus Cysteine Protease Inhibitors

Anirban Ghoshal[1], Álvaro F. Magalhães[2], Kesatebrhan Haile Asressu[1], Mohammad Anwar Hossain[1], Matthew H. Todd[2] and Timothy M. Willson[1]*

[1] Structural Genomics Consortium, UNC Eshelman School of Pharmacy, University of North Carolina at Chapel Hill, Chapel Hill, NC 27599, USA.

[2] Structural Genomics Consortium, Department of Pharmaceutical and Biological Chemistry, University College London School of Pharmacy, London, WC1N 1AX, UK.

* Correspondence: tim.willson@unc.edu

Abstract: Optimized syntheses of (*E*)-5-(2-ethoxyphenyl)-*N*-(3-(methylsulfonyl)allyl)-1*H*-pyrazole-3-carboxamide (RA-0002034, **1**), a promising antiviral covalent cysteine protease inhibitor lead, were developed. The syntheses avoid the contamination of **1** with the cyclic dihydropyrazolo[1,5-*a*]pyrazin-4(5*H*)-one **2**, which formed by intramolecular aza-Michael reaction of the vinyl sulfone warhead under basic conditions and at pH 7.4 in phosphate buffer. **1** could be synthesized using either modified amide coupling conditions or through introduction of a MOM-protecting group and was stable as a TFA or HCl salt. Although acyclic **1** demonstrated poor pharmacokinetics with high in vivo clearance in mice, the cyclic **2** showed improved plasma exposure. The potential use of dihydropyrazolo[1,5-*a*]pyrazin-4(5*H*)-ones as prodrugs for the acyclic β-amidomethyl-vinyl sulfone warhead was demonstrated by GSH capture experiments.

Graphical Abstract

RA-0002034, **1**
nsP2 protease
IC$_{50}$ = 60 nM

2
nsP2 protease
inactive
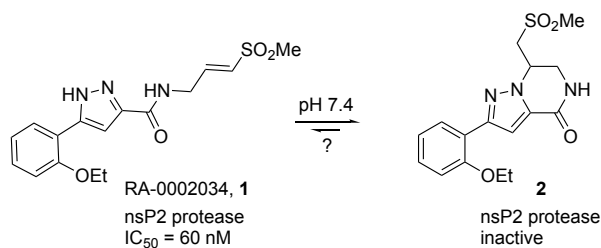
1. Introduction

Alphaviruses, a group of widespread, enveloped, single-stranded positive sense RNA viruses, are transmitted by Aedes aegypti and Aedes albopictus mosquitoes, posing a significant threat to public health [1]. These viruses are divided into two categories based on their geographical emergence: Old World alphaviruses, including chikungunya virus (CHIKV), Ross River virus (RRV), and O'nyong-nyong virus (ONNV) that typically present with rash, fever, and prolonged arthralgia that can persist for months post-infection [2]; and New World alphaviruses, including Venezuelan (VEEV), Western (WEEV) and Eastern (EEEV) Equine Encephalitis viruses and Mayaro virus (MAYV) that often result in encephalitis-like neurological symptoms, accompanied by fever, headache, and nausea, which can be fatal with 30–50% of EEEV cases resulting in mortality [3]. Despite the severity of these diseases, there are currently no FDA-approved drugs for any alphavirus-caused disease, highlighting the urgent need for the development of alphavirus therapeutics.
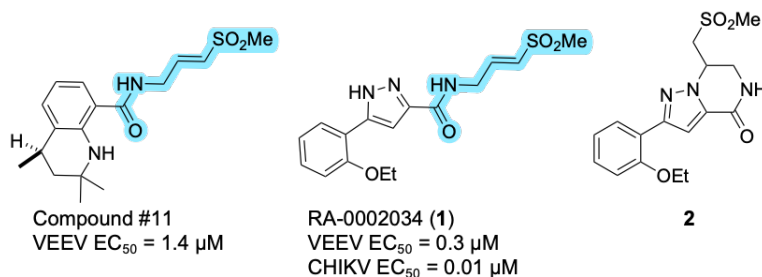

Figure 1. Alphavirus nsP2 protease inhibitors. The vinyl sulfone covalent warhead in compound #11 and RA-0002034 (**1**) is highlighted in blue. Potencies for inhibition of alphavirus replication are indicated.

The largest non-structural protein in the alphavirus genome, nsP2, is essential for viral replication [4]. nsP2 contains a C-terminal cysteine protease that uses a catalytic dyad of cysteine and histidine residues to catalyze substrate cleavage. Two covalent inhibitors of alphavirus nsP2 protease that contain a common β-amidomethyl-vinyl sulfone warhead have been recently disclosed (Figure 1). Compound #11 was reported as a micromolar inhibitor of VEEV nsP2 protease activity with antiviral activity [5]. Likewise, we reported the discovery of RA-0002034 (**1**) as potent covalent inhibitor CHIKV nsP2 protease with IC_{50} = 60 nM [6]. Vinyl sulfone **1** inhibited VEEV and CHIKV replication with EC_{50} = 0.3 and 0.01 μM, respectively, and decreased viral titer across a wide range of New and Old World alphaviruses [6]. Notably, the 5-arylpyrazole in **1** conferred an increase in potency for nsP2 protease inhibition compared to the

1,2-dihydroquinoline in Compound #11 demonstrating the importance of the heterocyclic amide substituent in molecular recognition by the viral protease.

Vinyl sulfones have broad utility as covalent inhibitors of cysteine proteases beyond viral nsP2 [7]. However, the cysteine reactivity of these warheads must be balanced with concerns of toxicity due to off-target activity or poor pharmacokinetics due to systemic GSH reactivity. During the resynthesis of **1** we observed the formation of a cyclic byproduct **2** that effectively masked the vinyl sulfone warhead. In this report we document methods to synthesize pyrazole-substituted β-amidomethyl-vinyl sulfones, such as **1**, devoid of contamination from cyclic dihydropyrazolo[1,5-*a*]pyrazin-4(5*H*)-ones. We also explored the reversibility of the cyclization reaction as a potential prodrug strategy for the cysteine-reactive acyclic β-amidomethyl-vinyl sulfone.

2. Results and Discussion

2.1. Identification of a Cyclic Product of Pyrazole-substituted β-Amidomethyl-vinyl Sulfone **1**

Synthesis of nsP2 protease inhibitor (*E*)-5-(2-ethoxyphenyl)-*N*-(3-(methylsulfonyl)allyl)-1*H*-pyrazole-3-carboxamide (**1**) from 3-carboxypyrazole (**3**) was attempted by amide coupling with (*E*)-3-(methylsulfonyl)prop-2-en-1-amine **4** using hexafluorophosphate benzotriazole tetramethyl uronium (HBTU), 1-hydroxybenzotriazole (HOBt), and diisopropylethylamine (DIPEA) in dimethylformamide (DMF). ^{1}H NMR analysis of the isolated product indicated an approx. 1:1 mixture of the expected product **1** together with a byproduct **2** that was inseparable by thin layer and column chromatography (Scheme 1).
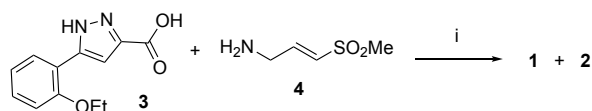
Scheme 1. (i) HBTU, HOBt, DIPEA, DMF, 25 °C, 16 h.

LCMS analysis using an Ultrahigh Performance Liquid Chromatography (UPLC) reverse phase column with an extended run time achieved baseline separation of **1** and **2** (Figure 2A). The mass spectra of the respective peaks showed predicted molecular weights of 349 Da for both compounds (Figure 2B and 2C), indicating that they were likely to be constitutional isomers. Preparative HPLC separation using a reverse phase Luna 5 μm phenyl-hexyl column (Phenomenex) provided high purity (>99%) samples of **1** and **2** as their TFA salts. CHIKV nsP2

4

protease inhibition was found to reside exclusively in **1** (IC_{50} = 60 nM) with the byproduct **2** devoid of activity in the enzyme assay at 100 µM [6].
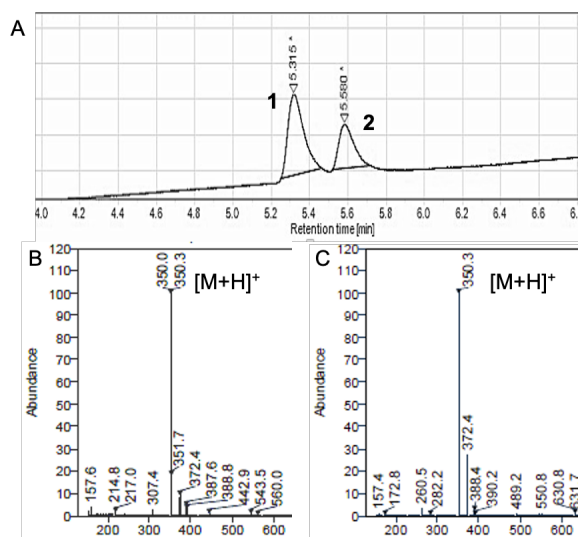

Figure 2. LCMS analysis of **1** and byproduct **2**. A. Analytical UPLC separation of **1** and **2** using reverse phase C18 2.7 µm column (Agilent). B. Positive ion mass spectrum of **1**, *m/z:* [M+H]$^+$ = 350. C. Positive ion mass spectrum of **2**, *m/z:* [M+H]$^+$ = 350.

Using a combination of ^{1}H and ^{13}C NMR spectroscopy, the chemical structure of **2** was determined to be a dihydropyrazolo[1,5-*a*]pyrazin-4(5*H*)-one (Figure 1) arising from intramolecular cyclization of **1**. ^{1}H NMR analysis of **1** showed characteristic olefinic protons corresponding to the (*E*)-vinyl sulfone at δ 6.69 ppm (dt, *J* = 15.3, 1.8 Hz, H14) and δ 6.82 ppm (dt, *J* = 15.3, 4.4 Hz, H13) (Figure 3A). These olefin resonances were absent in **2** (Figure 3B) and were replaced by a multiplet at δ 5.07 ppm (m, *J* = 8.9, 4.5 Hz, H9) and signals for two protons at δ 3.76-3.72 ppm (m, H11) and δ 3.98 ppm (dd, *J* = 14.4, 3.9 Hz, H11). Other resonances consistent with the cyclic structure of **2** were the non-equivalent methylene protons at δ 3.70 ppm (td, *J* = 6.3, 3.5 Hz, H8) and δ 3.93 ppm (ddd, *J* = 13.3, 4.4, 2.3 Hz, H8) (Figure 3B), which appeared as a single multiplet at δ 4.11 ppm in acyclic **1** (Figure 3A, H12). Additional evidence for the cyclic structure of **2** was provided by a ^{1}H-^{13}C heteronuclear multiple bond correlation (HMBC) experiment (Figure 3C) that indicated a three-bond correlation between atoms H9 and C7 in **2** that was absent in the acyclic **1**.
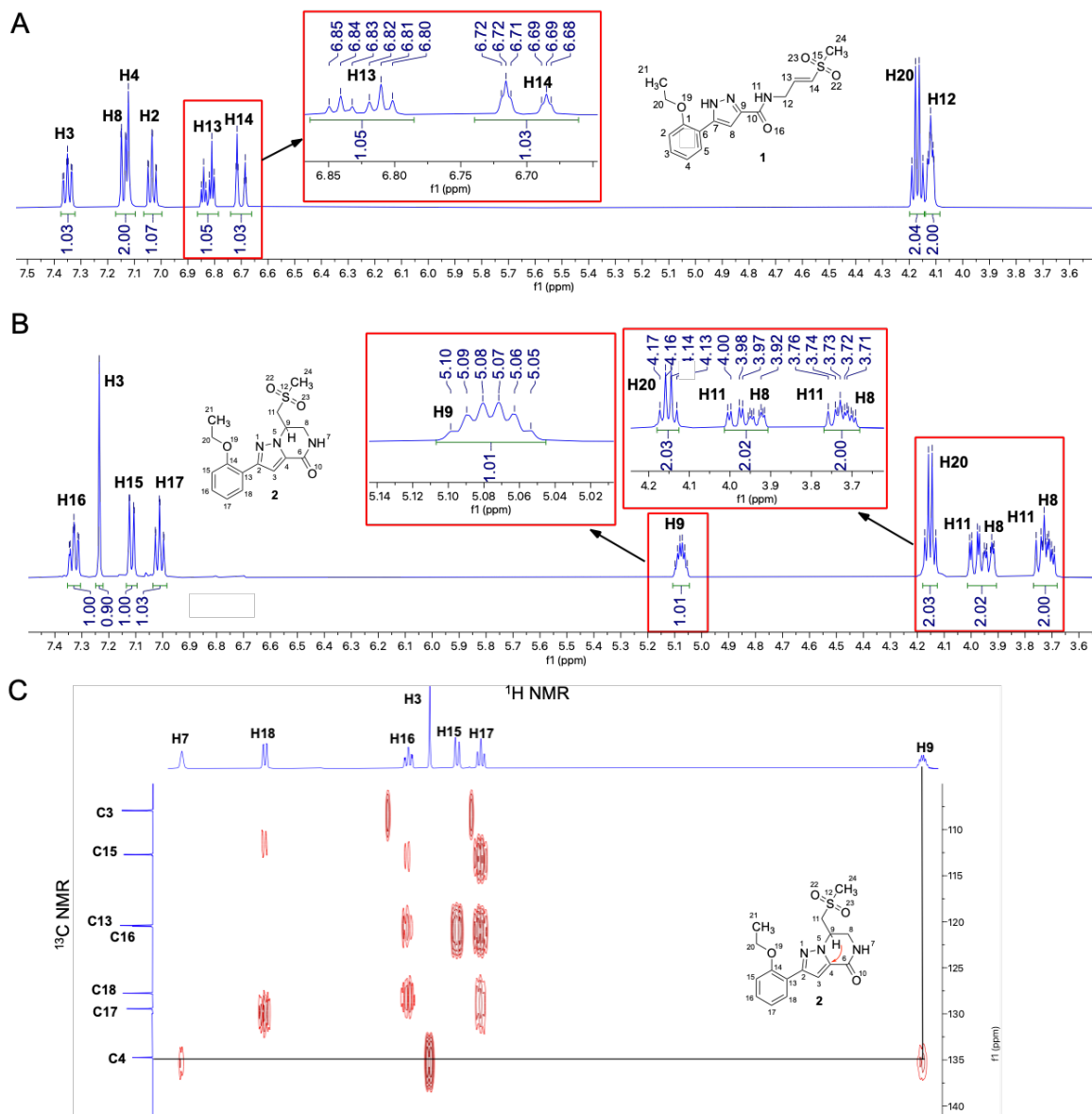
Figure 3. A. 500 MHz ^{1}H NMR spectra in DMSO-d_6. **1** has diagnostic olefin signals H13 and H14. B. **2** has diagnostic methine signal H9 and methylene signals for H8 and H11. C. ^{1}H-^{13}C HMBC spectrum of **2** indicating the three-bond correlation between atoms H9 and C4.

Formation of **2** is proposed to occur under the basic conditions of the amide coupling by a formal aza-Michael conjugate addition [8,9] of the pyrazole N2 into the β-carbon of the vinyl sulfone (Scheme 2). The resulting dihydropyrazolo[1,5-*a*]pyrazin-4(5*H*)-one, which masks the reactive vinyl sulfone warhead within its cyclic structure, was stable under normal laboratory conditions with no propensity to revert to the acyclic **1** upon storage as a solid or as a 10 mM DMSO stock solution. However, researchers are cautioned that commercial samples of **1** or other heterocyclic β-amidomethyl-vinyl sulfones (ChemSpace, Enamine) may contain undetermined

quantities of the respective dihydropyrazolo[1,5-*a*]pyrazin-4(5*H*)-ones unless careful quality control by ^{1}H NMR and UPLC analysis has been performed.
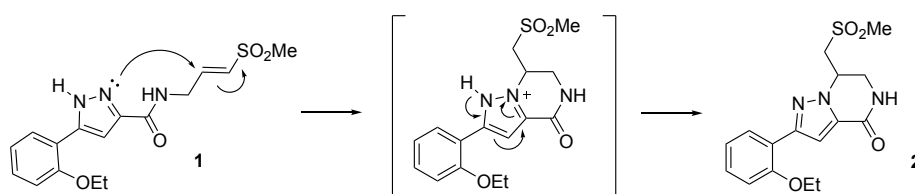
Scheme 2. Proposed mechanism of cyclization of **1** to **2**.

2.2. Stability of *1* in neutral phosphate buffer

To assess if cyclization of **1** into **2** could occur during the assessment of cellular antiviral activity, the stability of **1** in neutral pH phosphate buffer was investigated. To achieve this, a stock solution of **1** was prepared in DMSO-*d₆* and diluted into pH 7.4 phosphate buffer (with 10% D_2O) to a final concentration of 2 mM, in the presence of maleic acid as an internal standard. The solution was analyzed by ^{1}H NMR spectroscopy over 48 h at room temperature (Figure 4). At t = 1 h, vinyl sulfone **1** was present in solution at the expected 2 mM concentration. After 24 h, a reduction in the abundance of **1** by 10% and the appearance of approximately 9% of its cyclic isomer **2** was observed. After 48 h, 81% of **1** remained with approximately 19% of **2** present in the phosphate buffer.
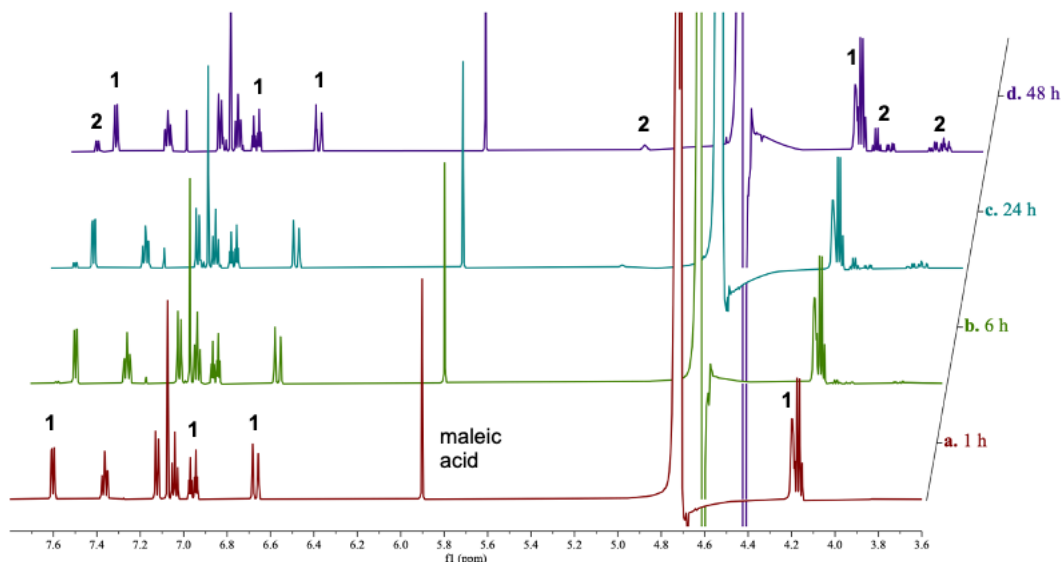

Figure 4. Cyclization of **1** in aqueous media. ^{1}H NMR (600 MHz, H_2O/D_2O 9:1, noesygppr1d, 3.6–7.8 ppm) of vinyl sulfone (**1**, 2 mM) in phosphate buffer (pH 7.4, 200 mM), with maleic acid (1 mM) as an internal standard after: **a.** 1 h; **b.** 6 h; **c.** 24 h; **d.** 48 h. Diagnostic signals for **1** and **2** are indicated.

7

These results demonstrated that partial cyclization of **1** into **2** might occur under standard cell culture conditions. Whether this decrease in the effective concentration of **1** would influence its efficacy as an antiviral nsP2 inhibitor would depend on the frequency of dosing and time course of the bioassay.

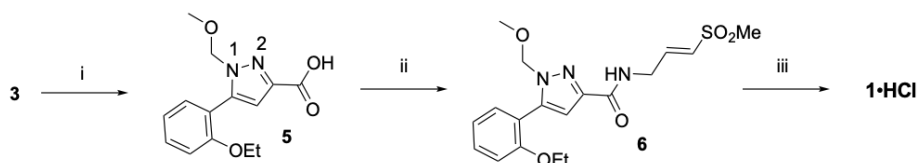### 2.3. *Optimized Synthesis of β-Amidomethyl-vinyl Sulfone* **1**

Alternative amide coupling conditions [10] were explored for the synthesis of acyclic β-amidomethyl-vinyl sulfone **1** that would avoid the formation of cyclic byproduct **2** and the subsequent preparative HPLC separation (Table 1). The original conditions using HBTU as the coupling agent and DIPEA as the base in DMF yielded a 60:40 mixture of **1** and **2** by analytical UPLC analysis (entry 1, Table 1). Switching the coupling agent to hexafluorophosphate azabenzotriazole tetramethyl uronium (HATU) or benzotriazol-1-yl-oxytripyrrolidino-phosphonium hexafluorophosphate (PyBOP) resulted in a similar ratio of **1** and **2** (entries 2 and 3). Use of n-propanephosphonic acid anhydride (T3P) as the coupling agent with triethylamine (TEA) as the base also yielded a 60:40 ratio of **1** and **2**, as did *N,N′*-diisopropylcarbodiimide (DIC) with 4-dimethylaminopyridine (DMAP) (entries 4 and 5). Each of these amide coupling reactions (entries 1–5) occurred in the presence of strongly basic amines with pK_a 9.7–10.9. Switching to 1-ethyl-3-(3-dimethylaminopropyl)carbodiimide (EDC) in combination with hydroxybenzotriazole (HOBt), where amide coupling occurs without the addition of an amine base resulted in an improved 70:30 ratio of **1** and **2** (entry 6). This result prompted us to trial the amide synthesis with the original benzotriazole tetramethyl uronium coupling agent but as a tetrafluoroborate salt (TBTU) in pyridine as a solvent. Under these less basic conditions (entry 7) exclusive formation of **1** was observed by UPLC analysis.

Table 1. Optimization of Amide Coupling between **3** and **4**[a]

Entry	Coupling Agent	Base	pK_a	Solvent	Temp (°C)	Time (h)	Ratio of 1:2[b]
1	HBTU	DIPEA	10.9	DMF	25	16	60:40
2	HATU	DIPEA	10.9	DMF	25	2	60:40
3	PyBOP	DIPEA	10.9	DMF	25	16	60:40
4	T3P	TEA	10.7	DMF	25	2	60:40
5	DIC	DMAP	9.7	DMF	25	16	60:40
6	EDC	HOBt	4.6	MeCN	25	2	70:30
7	TBTU	Pyridine	5.2	Pyridine	25	2	100:0

[a]Reaction conditions: **3** (1.0 eq.), **4** (1.2 eq.), solvent (0.2 M). [b]Quantified by analytical UPLC analysis.

An alternate synthesis of β-amidomethyl-vinyl sulfone **1** was also developed to avoid the liability of cyclization during the amide bond formation (Scheme 3). MOM-protection of pyrazole **3** occurred exclusively at the N1 position as expected [11,12] and was confirmed by ^{1}H-^{13}C HMBC NMR analysis. Coupling of MOM-protected pyrazole **5** using the TBTU-pyridine protocol gave exclusively amide **6** with no byproducts resulting from cyclization. Acid mediated cleavage of the MOM protecting group yielded pure **1** as an HCl salt without the need for chromatography. The HCl salt of **1** was stable upon storage as a solid or as a 10 mM DMSO stock solution.

Scheme 3. (i) MOMCl, K_2CO_3, DMSO (ii) **5**, TBTU, pyridine (iii) HCl, dioxane.

2.4. Optimized Synthesis of Dihydropyrazolo[1,5-a]pyrazin-4(5H)-one 2

Conditions for controlled cyclization of the HCl salt of β-amidomethyl-vinyl sulfone **1** to dihydropyrazolo[1,5-*a*]pyrazin-4(5*H*)-one **2** by intramolecular aza-Michael reaction were explored (Table 2). Reactions were performed at room temperature for 2h in the presence of different bases with the conversion to **2** monitored by UPLC. K_2CO_3 in ethanol gave efficient cyclization (entry 1). However, no cyclization occurred with K_2CO_3 in water due to the limited aqueous solubility of **1** (entry 2). Na_2CO_3 in an aqueous dioxane mixture resulted in clean cyclization to **2** (entry 3). The less basic $NaHCO_3$ in methanol or water was not as effective as K_2CO_3 (entries 4 and 5) within the 2h reaction time. The amine base TEA in methanol was also less effective (entry 6). The stronger amine bases DIPEA or DBU showed faster conversion to **2** but were still not as rapid as the inorganic bases (entries 7 and 8). Na_2CO_3 in an aqueous dioxane

Table 2. Optimization of Intramolecular Cyclization of **1** to **2**.

Entry	Base	Eq.	Solvent	Ratio of 1:2[b]
1	K_2CO_3	3.5	EtOH	0:100
2	K_2CO_3	3.5	H_2O	100:0
3	Na_2CO_3	3.0	Dioxane/H_2O	0:100
4	$NaHCO_3$	3.0	MeOH	12:88
5	$NaHCO_3$	3.0	H_2O	47:53
6	TEA	3.0	MeOH	51:49
7	DIPEA	3.0	DMF	4:96
8	DBU	0.5	ACN	8:92

[a]Reaction conditions: 25 °C, 2 h. [b]Quantified by analytical UPLC analysis.

(entry 3) was chosen as the optimal cyclization conditions for synthesis of **2** since it was fast, resulted in a simple work-up, and avoided the need for chromatography.

2.5.Pharmacokinetic Properties of *1* and *2*

Although vinyl sulfones have been used as covalent warheads for inhibition of a wide range of cysteine proteases [7], there are relatively few reports of their use in vivo [13]. To explore the potential of **1** as a drug lead for treatment or prevention of alphavirus infections, pharmacokinetic experiments were performed in mice following a 10 mg/kg i.v. dose (Figure 5).
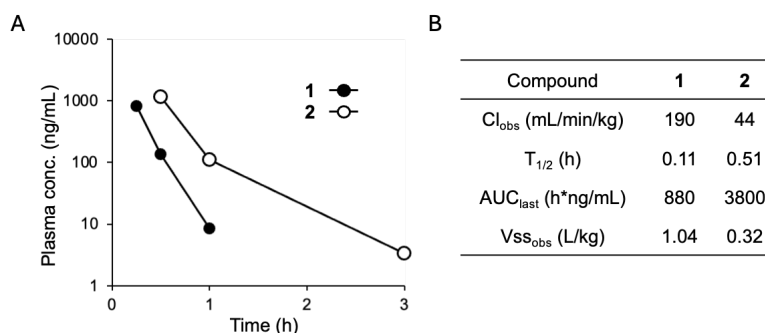

A.

B.

Compound	**1**	**2**
Cl_{obs} (mL/min/kg)	190	44
$T_{1/2}$ (h)	0.11	0.51
AUC_{last} (h*ng/mL)	880	3800
Vss_{obs} (L/kg)	1.04	0.32

Figure 5. Pharmacokinetics of 10 mg/kg i.v. dose of **1** or **2** in mice. A. Pooled plasma concentrations. B. Calculated pharmacokinetic parameters.

Unfortunately, β-amidomethyl-vinyl sulfone **1** had very rapid clearance with plasma levels falling below the limit of MS detection after 1h. From the observable data points the plasma half-life was calculated as only ~10 min. As a control, the pharmacokinetics of the cyclic dihydropyrazolo[1,5-*a*]pyrazin-4(5*H*)-one **2** were also determined (Figure 2). In comparison to **1**, the cyclic pyrazole **2** showed reduced plasma clearance with an i.v. half-life ~30 min and a 4-fold greater calculated plasma exposure. The rapid clearance of **1** compared to **2** suggested that the covalent β-amidomethyl-vinyl warhead was a liability for in vivo exposure in mice. Conversely, the improved exposure and reduced clearance of the dihydropyrazolo[1,5-*a*]pyrazin-4(5*H*)-one **2** raised the question of whether it might function as a prodrug for the reactive β-amidomethyl-vinyl sulfone **1** if the aza-Michael reaction was reversible.

2.6. Reversibility of the Aza-Michael Reaction

Cyclization of **1** to **2** was favored under basic conditions and **2** but occurred slowly at physiological pH. We were eager to determine if the cyclization was reversible and whether dihydropyrazolo[1,5-*a*]pyrazin-4(5*H*)-one **2** could revert to the acyclic β-amidomethyl-vinyl sulfone **1** by a retro-Michael reaction (Scheme 4).
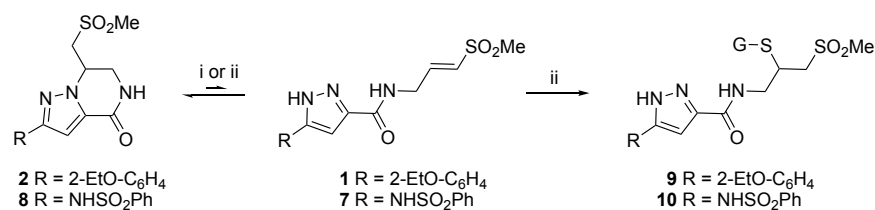
Scheme 4. (i) NaHCO$_3$ (1.0 eq.), MeOH, 25 °C. (ii) GSH (100x), phosphate buffer pH 7.4, 30 °C

The stability of the dihydropyrazolo[1,5-*a*]pyrazin-4(5*H*)-one **2** under standard laboratory conditions suggested that equilibrium with the acyclic β-amidomethyl-vinyl sulfone **1** lay predominantly toward the cyclic form. For example, **1** was below the limits of UPLC detection in 10 mM DMSO stock solutions of **2** even after prolonged storage over several months. Since low levels of the electrophilic β-amidomethyl-vinyl sulfone could theoretically still be present, we decided to test whether **1** could be captured using glutathione (GSH). Incubation of **1** with a 100-fold excess of GSH in phosphate buffer at 30 °C led to complete conversion to GSH adduct **9** within 8 h as monitored by LCMS (Table 3 and Figure S1). In contrast, incubation of dihydropyrazolo[1,5-*a*]pyrazin-4(5*H*)-one **2** with excess GSH did not result in formation the GSH adduct **9** even after 24 h. The GSH capture data demonstrated that no detectable level of the acyclic β-amidomethyl-vinyl sulfone **1** was present in phosphate buffer, making it extremely unlikely that dihydropyrazolo[1,5-*a*]pyrazin-4(5*H*)-one **2**, despite its improved pharmacokinetic properties, would be useful as a prodrug for **1**.

Notably, during structure-activity studies of the pyrazole β-amidomethyl-vinyl sulfones, a phenylsulfonamide-5-substituted pyrazole analog **7** was synthesized that appeared to be less prone to intramolecular cyclization. Under cyclization conditions of NaHCO$_3$ (1.0 eq.) in MeOH **1** was 100% converted to **2** in 36 h, but under the same conditions only ~50% of **7** cyclized to **8**. These results suggested that the structure of the pyrazole could influence the rate of aza-Michael cyclization and the propensity for the reverse reaction. To explore this possibility, an additional series of GSH capture experiments was performed. Incubation of β-amidomethyl-vinyl sulfone **7** with a 100-fold excess of GSH in phosphate buffer at 30 °C led to formation of its corresponding GSH adduct **10**, although conversion was slower than was seen with **1** and required 24 h to complete. More importantly, incubation of the corresponding dihydropyrazolo[1,5-*a*]pyrazin-4(5*H*)-one **8** with GSH resulted in the formation of 3% of the GSH adduct **10** after 8 h and 6% after 24 h (Figure S1). These results demonstrate that the cyclic dihydropyrazolo[1,5-*a*]pyrazin-4(5*H*)-one **8** exists in equilibrium with the acyclic β-amidomethyl-vinyl sulfone **7** in phosphate

11

buffer and adds credence to the potential use of dihydropyrazolo[1,5-*a*]pyrazin-4(5*H*)-ones as prodrugs for their corresponding cysteine reactive vinyl sulfones.

Table 3. Reversibility of the aza-Michael cyclization by GSH capture of the acyclic vinyl sulfones

| Time (h) | GSH-adduct formation (%)[a] | | | |
| | Acyclic | | Cyclic | |
	1	**7**	**2**	**8**
8	100	93	0	3
24	100	100	0	6

[a]Reaction conditions: GSH (100x), phosphate buffer, 30 °C

In conclusion, (*E*)-5-(2-ethoxyphenyl)-*N*-(3-(methylsulfonyl)allyl)-1*H*-pyrazole-3-carboxamide (RA-0002034, **1**) is a covalent inhibitor of nsP2 cysteine proteases with potent antiviral activity against New and Old World alphaviruses. Although **1** was prone to intramolecular cyclization to a cyclic dihydropyrazolo[1,5-*a*]pyrazin-4(5*H*)-one **2** under basic conditions and in phosphate buffer, two modified procedures were developed for the synthesis of the pure acyclic β-amidomethyl-vinyl sulfones as their TFA or HCl salts that can be employed in analog development for structure-activity studies of nsP2 protease inhibitors. The primary liability of **1** as an anti-alphavirus drug lead was its poor pharmacokinetics due to very high clearance in mice, which prompted us to explore the use of dihydropyrazolo[1,5-*a*]pyrazin-4(5*H*)-one **2** as a potential prodrug. Although cyclic **2** showed no evidence for retro aza-Michael reaction to give **1**, the phenylsulfonamide-5-substituted pyrazole **8** formed detectable levels of its acyclic β-amidomethyl vinyl sulfone **7** as evidenced by capture with GSH. These results demonstrate that the dihydropyrazolo[1,5-*a*]pyrazin-4(5*H*)-one chemotype can function as a masked form of the cysteine-reactive β-amidomethyl vinyl sulfone. Synthesis of dihydropyrazolo[1,5-*a*]pyrazin-4(5*H*)-one analogs with substituents that further favor equilibrium with their acyclic vinyl sulfones may provide a new prodrug strategy for covalent inhibition of viral nsP2 cysteine proteases.

3. Materials and Methods

3.1. General Methods

All reactions were performed in oven-dried glassware under an atmosphere of dry N_2 unless otherwise stated. All reagents and solvents used were purchased from commercial sources and were used without further purification. No unexpected safety hazards were encountered during chemical synthesis. Analytical thin layer chromatography (TLC) was performed on pre-coated

silica gel plates, 200 μm with an F_{254} indicator. TLC plates were visualized by fluorescence quenching under UV light or by staining with iodine and $KMnO_4$. Column chromatography was performed using Teledyne ISCO's RediSep $R_f{}^®$ pre-loaded silica gel cartridges on a Biotage automated purification system. NMR spectra were collected in DMSO-d_6 on Bruker 400 MHz and 500 MHz spectrometers. All chemical shifts are reported in parts per million (ppm, δ units) and are referenced to the residual protons in the deuterated solvent. Coupling constant units are in Hertz (Hz). Splitting patterns are indicated as follows: s (singlet), d (doublet), t (triplet), q (quartet), m (multiplet), dd (doublet of doublets), dt (doublet of triplets), td (triplet of doublets), ddd (doublet of doublets of doublets). Water suppressed ^1H NMR spectra were recorded at 298 K on a Bruker Avance Neo 600 MHz NMR spectrometer equipped with a QCI-F cryoprobe using a solvent suppression pulse sequence with pre-saturation and spoil gradients (1D spectra, noesygppr1d, Bruker) and chemical shifts (δ units) referenced to the residual water signal at 4.7 ppm. HRMS samples were analyzed with a Q Exactive HF-X (ThermoFisher, Bremen, Germany) mass spectrometer. Samples were introduced via a heated electrospray source (HESI) at a flow rate of 10 μL/min. HESI source conditions were set as: nebulizer temperature 400 °C, sheath gas (nitrogen) 20 arb, auxillary gas (nitrogen) 0 arb, sweep gas (nitrogen) 0 arb, capillary temperature 320 °C, RF voltage 45V. The mass range was set to 100-1000 m/z. All measurements were recorded at a resolution setting of 120,000. Solutions were analyzed at 0.1 mg/mL or less based on responsiveness to the ESI mechanism. Xcalibur (ThermoFisher, Breman, Germany) was used to analyze the data. Molecular formula assignments were determined with Molecular Formula Calculator (v 1.3.0). All observed species were singly charged, as verified by unit m/z separation between mass spectral peaks corresponding to the ^{12}C and $^{13}C^{12}C_{c-1}$ isotope for each elemental composition. Analytical LCMS data was obtained using a Waters Acquity UPLC system equipped with a photodiode array detector using the following method: solvent A = Water + 0.2% FA, solvent B = ACN + 0.1% FA, flow rate = 1 mL/min. The gradient started at 95% A for 0.05 min. Afterwards, it was ramped to 100% B over 2 min and held for an additional minute at this concentration before returning to 95% A. For extended LCMS runs, separations were conducted on an Agilent 1290 Infinity II LC System using an Agilent Infinity Lab PoroShell 120 EC-C18 column (30 °C, 2.7 μm, 2.1 × 50 mm). LC conditions were set at 95% water with 0.1% formic acid (A) ramped linearly over 15.1 mins to 100% acetonitrile with 0.1% formic acid (B) and held until 15.3 min. At 15.4 min the gradient was switched back to 95% A and allowed to re-equilibrate until

18.0 min. Injection volume for all samples was 4 uL. Preparative HPLC was performed using an Agilent 1260 Infinity II LC System equipped with a Phenomenex C18 column (PhenylHexyl, 30 °C, 5 μm, 75 x 30 mm) using the following method: Solvent A: water + 0.05% TFA; Solvent B: Acetonitrile; flow rate: 30.00 mL/min. LC conditions were set at 95% A ramped linearly over 26 min to 100% B and held until 28 min at 100% B. At 30 min the gradient was switched back to 95% A. Final compounds were determined to be ≥95% purity by analytical LCMS.

3.2. Optimized synthesis pyrazole vinyl sulfones (**1**, **7**) and dihydropyrazolo[1,5-*a*]pyrazin-4(5*H*)-ones (**2**, **8**)

(*E*)-5-(2-Ethoxyphenyl)-*N*-(3-(methylsulfonyl)allyl)-1*H*-pyrazole-3-carboxamide (**1**)

Method A: To a stirred solution of 5-(2-ethoxyphenyl)-1H-pyrazole-3-carboxylic acid (**3**, 100 mg, 0.43 mmol, 1.0 eq.) and TBTU (207 mg, 0.65 mmol, 1.5 eq.) in pyridine (3 mL), was added (*E*)-3-(methylsulfonyl)prop-2-en-1-amine (**4**, 89 mg, 0.52 mmol, 1.2 eq.) and the reaction was stirred at 25 °C for 2 h. On completion of the reaction based on TLC and LCMS analysis, the reaction was poured into water and extracted with EtOAc. The combined organic layers were dried over anhydrous Na_2SO_4, filtered, and concentrated to give the crude compound. Column chromatography (eluting with 0–100% EtOAc in hexanes) followed by preparative HPLC purification afforded the TFA salt of (*E*)-5-(2-ethoxyphenyl)-*N*-(3-(methylsulfonyl)allyl)-1*H*-pyrazole-3-carboxamide (**1**) as a white solid (140 mg, 70%): m.p. 70 °C; ^{1}H NMR (DMSO-d_6, 500 MHz): δ 8.62 (t, *J* = 5.9 Hz, 1H), 7.74 (dd, *J* = 7.6, 1.8 Hz, 1H), 7.34 (ddd, *J* = 8.5, 7.4, 1.7 Hz, 1H), 7.16 – 7.10 (m, 2H), 7.03 (td, *J* = 7.5, 1.1 Hz, 1H), 6.82 (dt, *J* = 15.2, 4.4 Hz, 1H), 6.69 (dt, *J* = 15.2, 1.8 Hz, 1H), 4.16 (q, *J* = 6.9 Hz, 2H), 4.11 (ddd, *J* = 6.1, 4.4, 1.8 Hz, 2H), 3.01 (s, 3H), 1.41 (t, *J* = 6.9 Hz, 3H); ^{13}C NMR (DMSO-d_6, 126 MHz): δ 161.5, 155.0, 143.5, 130.0, 129.7, 127.8, 120.6, 112.8, 105.6, 63.7, 42.2, 38.7, 14.6; HRMS (ESI) *m/z*: [M+H]$^+$ calculated for $C_{16}H_{20}N_3O_4S$: 350.1175; found 350.1172; HPLC purity >99%.

Method B: To a stirred solution of 5-(2-ethoxyphenyl)-1*H*-pyrazole-3-carboxylic acid (**3**, 1.0 g, 4.3 mmol, 1.0 eq.) in DMSO (10 mL) at 0°C were added K_2CO_3 (1.8 g, 13 mmol, 3.0 eq.) and chloromethyl methyl ether (0.39 mL, 5.2 mmol, 1.2 eq.) and the reaction was stirred at 25 °C for 1 h. On completion of the reaction based on TLC and LCMS analysis, the reaction was poured into water and extracted with Et_2O. The combined organic layers were washed with brine, dried over anhydrous Na_2SO_4, filtered, and concentrated to give the crude compound. Column

chromatography (eluting with 10% MeOH in CH$_2$Cl$_2$) afforded 5-(2-ethoxyphenyl)-1-(methoxymethyl)-1*H*-pyrazole-3-carboxylic acid (**5**) as a white solid (350 mg, 29%); ^{1}H NMR (DMSO-*d*$_6$, 500 MHz): δ 13.52 (s, 1H), 7.93 (dd, *J* = 7.7, 1.8 Hz, 1H), 7.37 (s, 1H), 7.33 (ddd, *J* = 8.3, 7.3, 1.8 Hz, 1H), 7.11 (dd, *J* = 8.4, 1.1 Hz, 1H), 7.01 (td, *J* = 7.4, 1.1 Hz, 1H), 5.77 (s, 2H), 4.15 (q, *J* = 6.9 Hz, 2H), 3.28 (s, 3H), 1.41 (t, *J* = 7.0 Hz, 3H); ^{13}C NMR (DMSO-*d*$_6$, 126 MHz): δ 160.4, 155.8, 146.7, 134.0, 129.6, 127.7, 120.5, 120.3, 112.9, 112.8, 80.2, 63.6, 56.3, 14.7; *m/z* [M+H]$^+$ 277.

To a stirred solution of **5** (200 mg, 724 µmol, 1.0 eq.) and TBTU (349 mg, 1.09 mmol, 1.5 eq.) in pyridine (5.0 mL) was added (*E*)-3-(methylsulfonyl) prop-2-en-1-amine (**4**, 149 mg, 869 µmol, 1.2 eq.) and the reaction was stirred at 25 °C for 2 h. On completion of the reaction based on TLC and LCMS analysis, the reaction was poured into water and extracted with EtOAc. The combined organic layers were dried over anhydrous Na$_2$SO$_4$, filtered, and concentrated to give the crude compound. Column chromatography (eluting with 0–100% EtOAc in hexanes) afforded (*E*)-5-(2-ethoxyphenyl)-1-(methoxymethyl)-*N*-(3-(methylsulfonyl)allyl)-1*H*-pyrazole-3-carboxamide (**6**) as a white solid (210 mg, 74%); ^{1}H NMR (DMSO-*d*$_6$, 500 MHz): δ 9.00 (t, *J* = 5.7 Hz, 1H), 7.90 (dd, *J* = 7.7, 1.8 Hz, 1H), 7.46 (s, 1H), 7.33 (ddd, *J* = 8.2, 7.3, 1.8 Hz, 1H), 7.12 (dd, *J* = 8.5, 1.1 Hz, 1H), 7.00 (td, *J* = 7.5, 1.1 Hz, 1H), 6.82 (dt, *J* = 15.3, 4.2 Hz, 1H), 6.74 (dt, *J* = 15.2, 1.6 Hz, 1H), 5.79 (s, 2H), 4.20 – 4.11 (m, 4H), 3.27 (s, 3H), 3.01 (s, 3H), 1.44 (t, *J* = 6.9 Hz, 3H); ^{13}C NMR (DMSO-*d*$_6$, 126 MHz): δ 159.2, 155.7, 146.6, 142.9, 136.0, 130.3, 129.5, 127.9, 120.8, 120.5, 112.9, 109.5, 79.9, 63.7, 56.3, 42.2, 38.9, 14.6; *m/z* [M+H]$^+$ 394.

To a stirred solution of **6** (100 mg, 254 µmol, 1.0 eq.) in CH$_2$Cl$_2$ was added 4M HCl in dioxane (1.3 mL, 5.1 mmol, 20.0 eq.) and the reaction was stirred at 25 °C for 3 h. On completion of the reaction based on TLC and LCMS analysis the reaction was concentrated. The resulting solid was washed with Et$_2$O and dried under high vacuum to obtain the HCl salt of (*E*)-5-(2-ethoxyphenyl)-*N*-(3-(methylsulfonyl)allyl)-1*H*-pyrazole-3-carboxamide (**1**) as a white solid (90 mg, 92%); m.p. 198 °C; HPLC purity >99%.

2-(2-Ethoxyphenyl)-7-((methylsulfonyl)methyl)-6,7-dihydropyrazolo[1,5-a]pyrazin-4(5*H*)-one (**2**)

To a stirred solution of (*E*)-5-(2-ethoxyphenyl)-*N*-(3-(methylsulfonyl)allyl)-1*H*-pyrazole-3-carboxamide (**1**, 100 mg, 286 µmol, 1.0 eq.) in 1,4-dioxane (1.5 mL) and water (1.5 mL) was added sodium carbonate (91.0 mg, 859 µmol, 3.0 eq.) and the reaction was stirred at 25 °C for 12 h. On

completion of the reaction based on LCMS analysis, the reaction was poured into water and extracted with EtOAc. The combined organic layers were dried over anhydrous Na_2SO_4, filtered, and concentrated to give the crude product. Column chromatography (eluting with 0–100% EtOAc in hexanes) afforded 2-(2-ethoxyphenyl)-7-((methylsulfonyl)methyl)-6,7-dihydropyrazolo[1,5-*a*]pyrazin-4(5*H*)-one (**2**) as a white solid (70 mg, 69%): m.p. 228 °C; ^{1}H NMR (DMSO-d_6, 500 MHz): δ 8.31 (t, J = 2.9 Hz, 1H), 7.95 (dd, J = 7.7, 1.8 Hz, 1H), 7.32 (ddd, J = 8.9, 7.4, 1.8 Hz, 1H), 7.23 (s, 1H), 7.11 (dd, J = 8.4, 1.0 Hz, 1H), 7.00 (td, J = 7.5, 1.0 Hz, 1H), 5.07 (dq, J = 9.0, 4.5 Hz, 1H), 4.15 (q, J = 7.0 Hz, 2H), 3.98 (dd, J = 14.4, 3.9 Hz, 1H), 3.93 (ddd, J = 13.3, 4.5, 2.4 Hz, 1H), 3.76 – 3.68 (m, 2H), 3.16 (s, 3H), 1.41 (t, J = 6.9 Hz, 3H); ^{13}C NMR (DMSO-d_6, 126 MHz): δ 158.1, 158.1, 155.7, 147.3, 134.8, 129.4, 127.8, 120.5, 120.4, 112.7, 107.9, 63.6, 53.8, 50.9, 43.0, 41.5, 14.7; HRMS (ESI) *m/z*: [M+H]$^+$ calculated for $C_{16}H_{20}N_3O_4S$: 350.1175; found 350.1177; HPLC purity >99%.

(*E*)-*N*-(3-(Methylsulfonyl)allyl)-5-(phenylsulfonamido)-1*H*-pyrazole-3-carboxamide (**7**)

To a stirred solution of 5-(phenylsulfonamido)-1H-pyrazole-3-carboxylic acid (184 mg, 688 μmol, 1.0 eq.) and TBTU (332 mg, 1.03 mmol, 1.5 eq.) in pyridine (5.0 mL), (*E*)-3-(methylsulfonyl) prop-2-en-1-amine (**4**, 142 mg, 0.83 mmol, 1.2 eq.) was added and the reaction was stirred at 25 °C for 2 h. On completion of the reaction based on TLC and LCMS analysis, the mixture was poured into water and extracted with EtOAc. The combined organic layers were dried over anhydrous Na_2SO_4, filtered, and concentrated to give the crude compound. Column chromatography (eluting with 0–100% EtOAc in hexanes), followed by preparative HPLC purification afforded the TFA salt of (*E*)-*N*-(3-(methylsulfonyl)allyl)-5-(phenylsulfonamido)-1*H*-pyrazole-3-carboxamide (**7**) as a white solid (125 mg, 36%): m.p. 181 °C; ^{1}H NMR (DMSO-d_6, 500 MHz): δ 13.17 (s, 1H), 10.64 (s, 1H), 8.86 (s, 1H), 7.80 – 7.77 (m, 2H), 7.63 (t, J = 7.3 Hz, 1H), 7.57 (t, J = 7.5 Hz, 2H), 6.82 – 6.69 (m, 3H), 4.07 (t, J = 4.7 Hz, 2H), 3.00 (s, 3H); ^{13}C NMR (DMSO-d_6, 126 MHz): δ 158.4, 145.9, 142.7, 140.1, 136.9, 132.8, 130.3, 129.1, 126.6, 97.3, 42.1, 38.7; HRMS (ESI) *m/z*: [M+H]$^+$ calculated for $C_{14}H_{17}N_4O_5S_2$ 385.0640; found 385.0577; HPLC purity > 98%.

N-(7-((Methylsulfonyl)methyl)-4-oxo-4,5,6,7-tetrahydropyrazolo[1,5-*a*]pyrazin-2-yl)benzenesulfonamide (**8**)

To a stirred solution of (*E*)-*N*-(3-(methylsulfonyl)allyl)-5-(phenylsulfonamido)-1*H*-pyrazole-3-carboxamide 2,2,2-trifluoroacetate (**7** , 50.0 mg, 100 μmol, 1.0 eq.) in 1,4-dioxane (1.5 mL) and water (1.5 mL) was added NaHCO$_3$ (25 mg, 300 μmol, 3.0 eq.) and the reaction was stirred at 25 °C for 12 h. On completion of the reaction based on LCMS analysis, the mixture was poured into water and extracted with EtOAc. The combined organic extracts were dried over anhydrous Na$_2$SO$_4$, filtered, and concentrated to give the crude compound. Column chromatography (eluting with 0–100% EtOAc in hexanes), followed by preparative HPLC purification afforded the TFA salt of *N*-(7-((methylsulfonyl)methyl)-4-oxo-4,5,6,7-tetrahydropyrazolo[1,5-*a*]pyrazin-2-yl)benzenesulfonamide (**8**) as a white solid (20.0 mg, 39%): m.p 222 °C; ^{1}H NMR (DMSO-*d$_6$*, 500 MHz): δ 10.97 (s, 1H), 8.29 (t, *J* = 2.8 Hz, 1H), 7.83 – 7.81 (m, 2H), 7.67 – 7.63 (m, 1H), 7.60 – 7.56 (m, 2H), 6.36 (d, *J* = 1.3 Hz, 1H), 4.82 (dq, *J* = 9.2, 4.7 Hz, 1H), 3.81 (ddd, *J* = 13.4, 4.5, 2.2 Hz, 1H), 3.65 (dd, *J* = 14.5, 4.6 Hz, 1H), 3.62 – 3.56 (m, 2H), 2.99 (s, 3H); ^{13}C NMR (DMSO-*d$_6$*, 176 MHz): δ 157.3, 145.9, 139.9, 135.0, 133.0, 129.3, 126.7, 97.9, 53.9, 50.5, 42.9, 41.4; ^{13}C NMR (DMSO-*d$_6$*, 214 MHz): δ 157.3, 145.9, 139.9, 135.0, 133.1, 129.3, 126.7, 97.9, 53.9, 50.5, 42.9, 41.5. HRMS (ESI) *m/z*: [M+H]$^+$ calculated for C$_{14}$H$_{17}$N$_4$O$_5$S$_2$ 385.0640; found 385.0584; HPLC purity > 98%.

3.3 ^{1}H NMR Stability Assay

A 40 mM stock solution of **1** in DMSO-*d$_6$* was prepared. A 95 mM stock solution of maleic acid was prepared in D$_2$O. The stock solutions of **1** (27.5 μL, 1.1 μmol) and maleic acid (5.8 μL, 0.55 μmol), were added to D$_2$O (49.2 μL) and pH 7.4 phosphate buffer (467.5 μL, 200 mM). The mixture was analysed periodically by ^{1}H NMR (600 MHz, H$_2$O/D$_2$O 9:1, noesygppr1d, 256 scans) and held at room temperature between NMR acquisitions.

3.4. Pharmacokinetic Methods

Male CD1 mice were dosed intravenously with 10 mg/kg solutions of **1** in DMSO/PEG-400/Water (v/v/v, 5/40/55) or **2** in NMP/Solutol/PEG-400/normal saline (10:5:40:45; v/v/v/v). Blood was collected at intervals of 0.25, 0.5, 1, and 3 h (for **1**) and 0.5, 1, 3, and 5 h (for **2**) post dose from the dorsal metatarsal vein and transferred into plastic micro centrifuge tubes containing anticoagulant of EDTA-K2. Blood samples were centrifuged at 4,000 g for 5 min at 4 °C to obtain plasma. The plasma samples from each time point were pooled and then analyzed by LCMS/MS. The PK parameters were estimated by non-compartmental model using WinNonlin 8.3.

3.5. GSH Capture Assay

A 10 mM solution of GSH (Sigma Aldrich Cat# G4251) was prepared in a pH 7.4 phosphate buffer. A 10 mM DMSO solution of test compound was diluted in phosphate buffer to give a solution at 100 µM with 1% DMSO. At time zero (t = 0), 50 µL of the 100 µM test compound solution was added to an Eppendorf tube containing 50 µL phosphate buffer and 50 µL of 10 mM GSH solution. The final concentration of the compound and GSH were maintained at 50 µM and 5 mM, respectively. The Eppendorf tube was vortexed and then the sample was transferred to a high recovery autosampler vial for LCMS analysis. Analysis was performed at 8 and 24 h time points and the percentage of GSH adduct formation was calculated using Agilent LCMS software.

Supplementary Materials: Figure S1: GSH Capture Spectra. Analytical data for **1**, **2**, **7** and **8**.

Author Contributions: Conceptualization, M.H.T. and T.M.W.; investigation, A.G., K.H.A, A.F.M, and A.H.; methodology, A.G. and A.F.M.; writing–original draft, M.H.T and T.M.W.; writing–review and editing, A.G., K.H.A, A.F.M, and M.H.T.

References

1. Skidmore, A.M.; Bradfute, S.B. The life cycle of the alphaviruses: From an antiviral perspective. *Antiviral Res* **2023**, *209*, 105476, doi:10.1016/j.antiviral.2022.105476.
2. Suhrbier, A.; Jaffar-Bandjee, M.C.; Gasque, P. Arthritogenic alphaviruses--an overview. *Nat Rev Rheumatol* **2012**, *8*, 420-429, doi:10.1038/nrrheum.2012.64.
3. Morens, D.M.; Folkers, G.K.; Fauci, A.S. Eastern Equine Encephalitis Virus - Another Emergent Arbovirus in the United States. *N Engl J Med* **2019**, *381*, 1989-1992, doi:10.1056/NEJMp1914328.
4. Abu Bakar, F.; Ng, L.F.P. Nonstructural Proteins of Alphavirus-Potential Targets for Drug Development. *Viruses* **2018**, *10*, doi:10.3390/v10020071.
5. Zhang, H.; Harmon, M.; Radoshitzky, S.R.; Soloveva, V.; Kane, C.D.; Duplantier, A.J.; Ogungbe, I.V. Vinyl Sulfone-Based Inhibitors of Nonstructural Protein 2 Block the Replication of Venezuelan Equine Encephalitis Virus. *ACS Med Chem Lett* **2020**, *11*, 2139-2145, doi:10.1021/acsmedchemlett.0c00215.
6. Merten, E.M.; Sears, J.D.; Leisner, T.M.; Hardy, P.B.; Ghoshal, A.; Hossain, M.A.; Asressu, K.H.; Brown, P.J.; Stashko, M.A.; Herring, L.E.; et al. Discovery of a cell-active chikungunya virus nsP2 protease inhibitor using a covalent fragment-based screening approach. *bioRxiv* **2024**, doi:10.1101/2024.03.22.586341.
7. Ahmadi, R.; Emami, S. Recent applications of vinyl sulfone motif in drug design and discovery. *Eur J Med Chem* **2022**, *234*, 114255, doi:10.1016/j.ejmech.2022.114255.
8. McDowell, S.T.; Stirling, C.J.M. Elimination–addition. Part X. Rates of addition of amines to p-tolyl vinyl sulphone. *J Chem. Soc. B* **1967**, 343-348.
9. McDowell, S.T.; Stirling, C.J.M. Elimination–addition. Part XI. Electronic effects upon the reactivity of aryl vinyl sulphones towards amines. *J Chem. Soc. B* **1967**, 348-350.
10. El-Faham, A.; Albericio, F. Peptide coupling reagents, more than a letter soup. *Chem Rev* **2011**, *111*, 6557-6602, doi:10.1021/cr100048w.
11. Almena, I.; Díz-Barra, E.; Hoz, A.D.L.; Ruiz, J.; Sínchez-Migallón, A.; Elguero., J. Alkylation and arylation of pyrazoles under solvent-free conditions: Conventional heating versus microwave irradiation. *J Heterocyclic Chem.* **1998**, *35*, 1263-1268.
12. Huang, A.; Orcid, W., K.; Lee, S.Y.C.; Kneitschel, N.; Chang, J.; Zhu, K.; Mello, T.; Bancroft, L.; Norman, N.J.; Zheng, S.-L. Regioselective Synthesis, NMR, and Crystallographic Analysis of N1-Substituted Pyrazoles. *J Org. Chem.* **2017**, *82*, 8864-8872.
13. Xiao, Y.C.; Chen, F.E. The vinyl sulfone motif as a structural unit for novel drug design and discovery. *Expert Opin Drug Discov* **2024**, *19*, 239-251, doi:10.1080/17460441.2023.2284201.